Isothermal crystallization of isotactic polypropylene in dotriacontane. III. Effect of dilution and crystallization temperature on growth rate

Yu F. Wang and Douglas R. Lloyd*
Department of Chemical Engineering, Center for Polymer Research, The University of Texas at Austin, Austin, TX 78712, USA
(Received 10 August 1992)

The spherulitic growth rate of isotactic polypropylene in dotriacontane was studied using optical microscopy. Polymer concentration was varied from 100 to 10 wt% iPP in 10 wt% intervals. Crystallization temperature was varied from 372 to 429 K in 1 K intervals. The influence of these variables on polymer spherulitic growth rate and regime transitions was analysed using the Lauritzen–Hoffman and Toda nucleation theories.

(Keywords: crystallization; isotactic polypropylene; kinetics)

INTRODUCTION

The Lauritzen and Hoffman (LH) surface nucleation theory for polymer crystallization is based on the following points[1,2]:

1. The chain folding character of polymer molecules is a kinetics-controlled phenomenon since the chain-folded structure is not in equilibrium with its environment.
2. Spherulite growth has a strong dependence on crystallization temperature, T_c.

The LH theory has been used to quantify polymer crystallization kinetics in the melt[1-10]. Although the LH theory was derived for pure homopolymers, the theory has also been applied to polymer blends[11-15] and single crystals in dilute solutions[16,17]. Other surface nucleation theories have been proposed to quantify the kinetics of melt crystallization[18] and dilute solution crystallization[10,19-21], but have not found widespread use. The objective of the study reported here was to evaluate the applicability of the LH theory over the concentration range 10–100% polymer. The model system isotactic polypropylene (iPP) and dotriacontane ($C_{32}H_{66}$) was studied using optical microscopy.

The LH theory indicates the crystal growth rate is characterized by three regimes that depend on T_c, or more specifically, supercooling (ΔT, defined as $T_m^\circ - T_c$, where T_m° is the equilibrium melting temperature). For polymer crystallized at small supercooling, lamellar growth is initiated by the deposit of a single nucleus on a substrate. Polymer molecules fold onto the substrate to complete a layer. The growth rate of polymer crystals, G, expressed in terms of length/time, can be formulated as[3]:

$$G = G_0 \exp\{-U^*/R(T_c - T_\infty)\} \exp(-4b\sigma\sigma_e T_m^\circ / k\Delta H T_c \Delta T f) \quad (1)$$

where:

G_0 is the pre-exponential factor;
b is the thickness of a monolayer (cm);
σ_e is the fold surface free energy (erg cm^{-2});
σ is the lateral surface free energy (erg cm^{-2});
ΔH is the polymer heat of fusion (erg cm^{-3});
k is the Boltzmann constant (erg K^{-1} mol^{-1});
T_c is the polymer crystallization temperature (K);
T_∞ is the temperature at which polymer crystallization ceases (K);
T_m° is the equilibrium melting temperature (K);
ΔT is the degree of supercooling, defined as $T_m^\circ - T_c$ (K);
U^* is the Williams, Landel and Ferry (WLF) shift constant (cal mol^{-1});
R is the gas constant (cal mol^{-1} K^{-1});
f is defined by $2T_c/(T_m^\circ + T_c)$.

The crystallization driving force is proportional to ΔT. When ΔT is increased, multiple nucleation occurs on the substrate and the crystallization rate enters regime II growth. In this regime, the growth rate is expressed as[20]:

$$G = G_0 \exp\{-U^*/R(T_c - T_\infty)\} \exp\{-2b\sigma\sigma_e T_m^\circ / k\Delta H T_c \Delta T f\} \quad (2)$$

When the supercooling is increased further, the average separation of nucleation sites is close to the polymer molecular stem width, and regime III growth occurs. In regime III, the final expression is similar to equation (1) except G_0 differs from that found in regime I[22].

Comparing equations (1) and (2), one obtains

$$G = G_0 \exp\{-U^*/R(T_c - T_\infty)\} \exp\{-K_g/T_c \Delta T f\} \quad (3)$$

or in logarithmic form

$$\ln G + U^*/R(T_c - T_\infty) = \ln G_0 - K_g/T_c \Delta T f \quad (4)$$

* To whom correspondence should be addressed

0032-3861/93/112324-06

where K_g is defined as

$$K_g = xb\sigma\sigma_e T_m^\circ / k\Delta H \quad (5)$$

with the value of x depending on the growth regime; x is 2 in regime II and 4 in regimes I and III. Thus, if $\ln G + U^*/R(T_c - T_\infty)$ is plotted against $T_m^\circ/T\Delta Tf$, a straight line should be obtained with slope K_g and intercept $\ln G_0$.

For iPP, $ab = 34.37\,\text{Å}^2$, $b = 6.26\,\text{Å}$ on the (1 1 0) growth plane, $\sigma = 11.5\,\text{erg cm}^{-2}$, length of monomer unit = 2.165 Å, and $\Delta H = 1.96 \times 10^9\,\text{erg cm}^{-3}$ (ref. 22). The value of x is equal to 2 or 4 when the regime under consideration is II or III, respectively. Hoffman found $T_\infty = T_g - 30\,\text{K}$ and $U^* = 1500\,\text{cal mol}^{-1}$ by fitting the crystallization kinetics rate data for various polymers[3]. In the iPP–$C_{32}H_{66}$ system, a value for T_g was estimated using the Fox equation:

$$1/T_{g(\text{mix})} = W_{PP}/T_{g(PP)} + W_{C32}/T_{g(C32)} \quad (6)$$

where W_i and T_{gi} are the mass fraction and glass transition temperature of component i, respectively.

Numerous homopolymers[3,23], including iPP[24–26], have been found to have growth rates in more than one regime.

The crystallization kinetics of polymer–diluent systems over wide concentration ranges has been studied[27–31]. However, little work has been done to study the effect of diluent on regime transition in dilute solution polymer crystallization[32–35]. Thus, a study of diluent effect on the crystallization kinetics and regime transition is warranted. The crystallization kinetics data of this work are quantitatively analysed using the LH theory. The results are qualitatively explained by LH, kinetic roughening surface growth (KRSG), and impurity theories developed by Hoffman, Lauritzen, Sadler and Gilmer[36–41] and Toda *et al.*[42].

MATERIALS AND METHODS

The materials used in this study have been described elsewhere[43]. A Brinkman Model R110 rotary evaporator was used to make samples for optical microscopy. All glassware was thoroughly cleaned by immersion in Alconox overnight, washed off with deionized water from a Mega Pure filtering system, and heated in a Blue M convection oven. Isotactic polypropylene (iPP) and dotriacontane ($C_{32}H_{66}$) were used without further purification. The *p*-xylene (Aldrich Chemical Co.) was vacuum distilled and the middle cut was collected in a round-bottomed 500 ml flask. iPP and $C_{32}H_{66}$ in appropriate weight proportions were added to a 250 ml boiling flask. The weight of iPP used for each batch was 0.10 g and the volume of *p*-xylene was 100 ml. The boiling flask was rotated and heated so that *p*-xylene began to boil and the iPP dissolved. Vacuum was applied to the boiling flask for 10 min upon boiling (to ensure the solution was homogeneous) to withdraw the *p*-xylene at a fast rate. A thin layer of precipitated polymer and diluent formed and was peeled off the flask after immersing the flask in water at room temperature.

The vapour pressure of $C_{32}H_{66}$ at 313 K (the boiling point of the system) is ≈ 0.307 Pa ($\approx 2.3 \times 10^{-3}$ mmHg) based on the known vapour pressure of nonacosane ($C_{29}H_{60}$) at 303 K; therefore, entrainment of $C_{32}H_{66}$ in the evaporating *p*-xylene should be minimal. Samples made by evaporation were wrapped in filter paper and $C_{32}H_{66}$ was extracted for 24 h using *p*-xylene. The mass balance was closed to within 0.5 wt% for samples of all concentrations.

The sample was mounted on a 2.2 × 2.2 cm glass slide cover (used as received) and heated on a Kofler hot stage at 493 K for 10 min. Preliminary studies showed iPP growth rate remained unchanged even for samples heated at 493 K for 1 h. Annealing conditions of 473 K for 10 min did not affect the growth rate of pure iPP.

The annealed sample was quickly transferred to a waiting Mettler FP82 hot stage at the desired crystallization temperature. The growth rate was monitored under an Olympus IMT2 inverted microscope equipped with ultralong working distance phase-contrast objectives. The image of the spherulite was projected to the side port of the microscope and picked up by a Dage-Mti video camera. The video signal was transferred through a coaxial cable to an Image Technology acquisition board. The signal was digitized and stored in an IBM AT computer for later analysis. The acquired image was analysed by measuring the spherulite radius as a function of time. The radius was measured with a digitizing tablet (Digi Pad). The measured spherulitic radius was plotted against time. The growth rate was taken as the slope of the linear portion of the plot, where linearity was defined as the range of data that gave a linear regression slope with coefficient $\geqslant 0.98$.

RESULTS AND DISCUSSION

The logarithm of growth rate, G, was plotted *versus* T_c in *Figure 1*. Regime II and III growth behaviour are observed for each sample. The procedure for determining the transition temperature or break point for each system was as follows.

(i) A likely break point was selected based on visual inspection of *Figure 1*.
(ii) Regression analysis was performed using the selected break point and all points extending to the right, including end point to the right of the selected break point.
(iii) The end point in (ii) was omitted in each subsequent regression until the number of points between the break point and end point was equal to four points.
(iv) The analysis in (ii) and (iii) was repeated with a new break point to the right or left by five points from the break point selected in (i).
(vi) Analysis similar to that described in (ii) through (iv) was performed using points to the left of the original break point in (i).
(v) The break point that yielded the best regression correlation coefficients to the right and left was selected.

The transition temperatures so established are indicated in *Table 1*.

For pure iPP, the growth rate plot appears to change slope at $T_c = 413$ K. For $T_c < 413$ K, crystal growth is in regime II and for $T_c > 413$ K, crystal growth is in regime III[22,26]. A similar trend was observed for the other samples in *Figure 1*. The break point moved to lower temperatures as the polymer concentration decreased. The trend can be understood in terms of the nucleation density in each of the two regimes. As the iPP was diluted by $C_{32}H_{66}$, the equilibrium melting temperature of the iPP was decreased; therefore, at a fixed T_c the

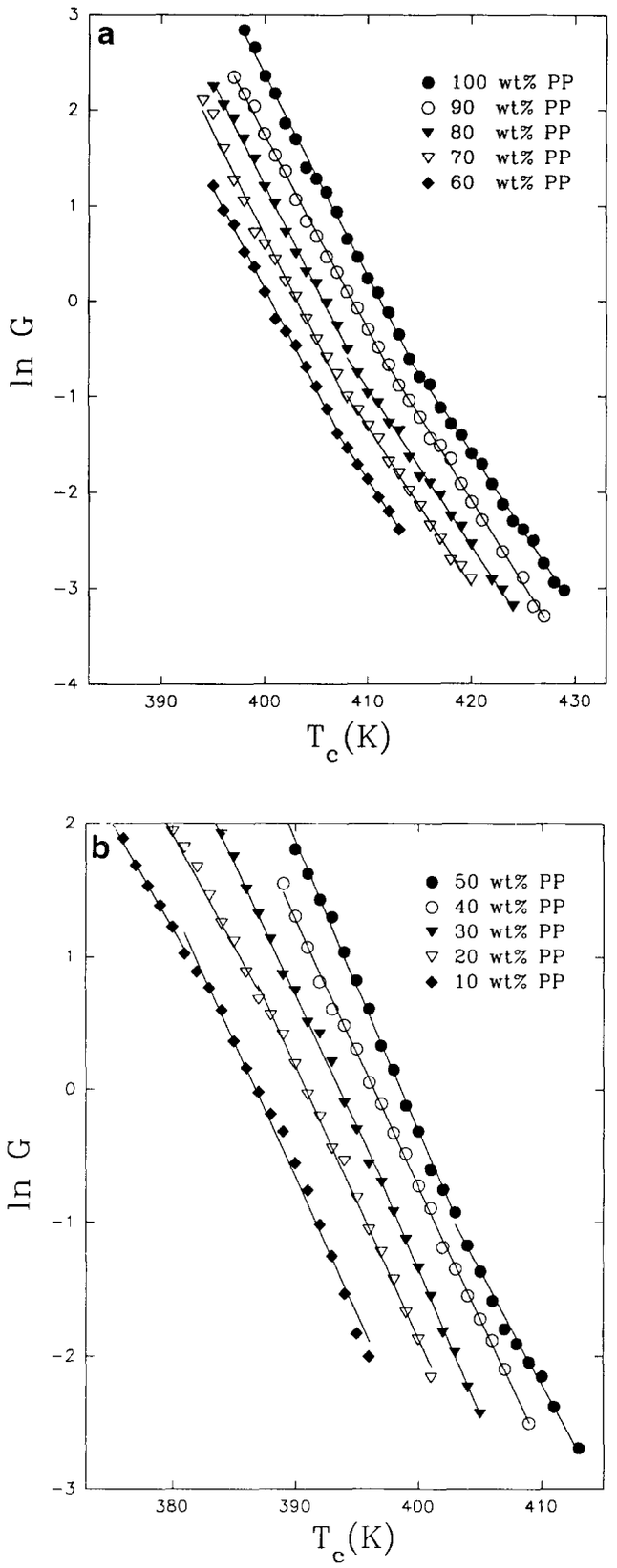

Figure 1 Growth rate data for iPP–$C_{32}H_{66}$ system. (a) 100 to 60 wt% iPP; (b) 50 to 10 wt% iPP

supercooling was reduced. Consequently, the nucleation density on the substrate decreased. The reduction in nucleation density made less nucleation sites available for further crystallization, which is characteristic of regime III to II transition. Thus, the regime transition temperature was lowered as the amount of diluent in the system increased.

The growth regime transition seemed to disappear at 40 wt% iPP but appeared again in the more dilute samples. At iPP concentration <40 wt%, the regime III slope at high T_c is smaller than the slope at low T_c. That is, the trend in *Figure 1* resembles a regime II to I transition in this concentration range. To be sure the

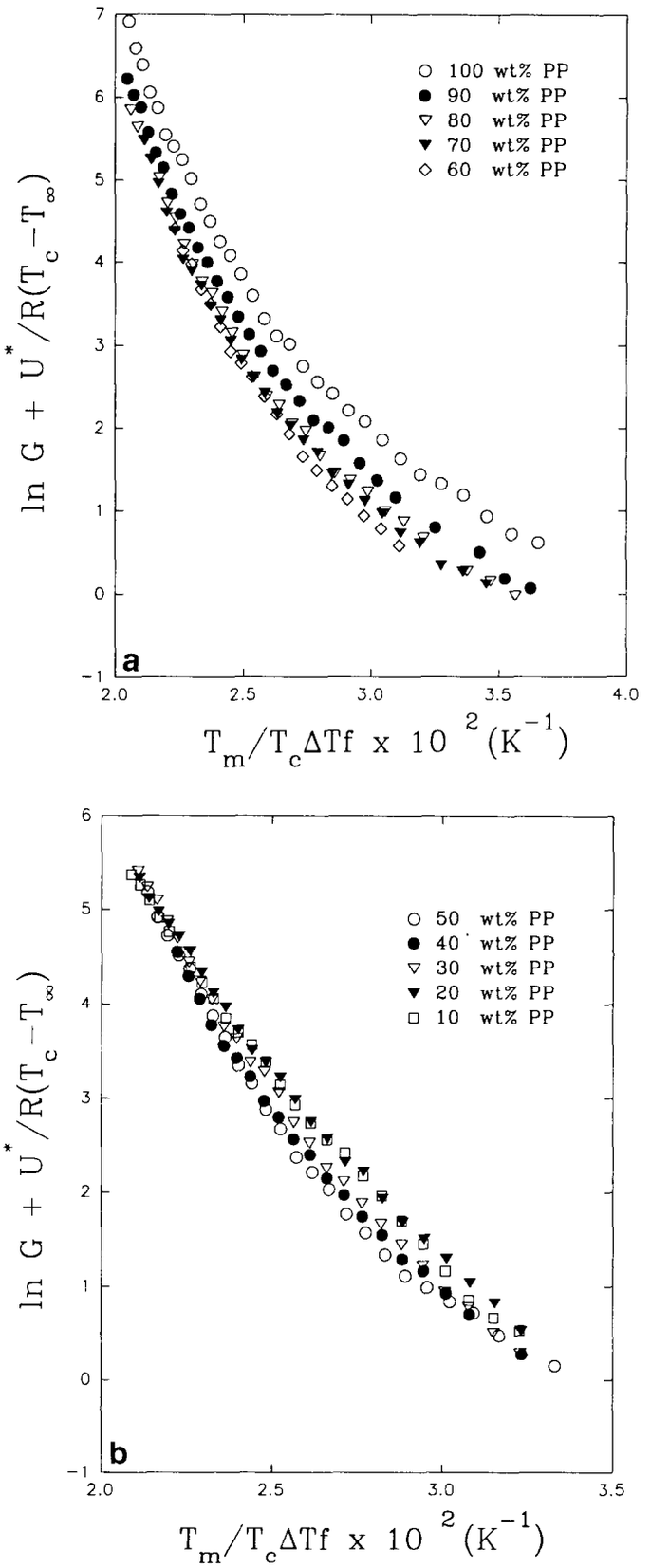

Figure 2 Lauritzen–Hoffman (LH) kinetic analysis based on the melting points obtained by the Hoffman–Weeks method. (a) 100 to 60 wt% iPP; (b) 50 to 10 wt% iPP

Table 1 Results of Lauritzen–Hoffman analysis

iPP (wt%)	Regime III			Regime II			
	Range (K)	$K_{g,III}$ $\times 10^5$ (K^2)	σ_e (erg cm^{-2})	Range (K)	$K_{g,II}$ $\times 10^5$ (K^2)	σ_e (erg cm^{-2})	$K_{g,III}/K_{g,II}$
100	402–414	2.785 ± 0.109	55.74 ± 2.22	414–424	1.403 ± 0.031	57.17 ± 1.26	1.98
90	401–411	2.732 ± 0.165	55.87 ± 3.37	413–423	1.386 ± 0.075	56.69 ± 3.06	1.96
80	402–410	2.564 ± 0.086	52.71 ± 1.76	410–420	1.286 ± 0.101	52.88 ± 4.15	1.99
70	397–408	2.471 ± 0.135	51.11 ± 2.81	408–418	1.280 ± 0.061	52.95 ± 2.52	1.93
60	395–407	2.410 ± 0.137	50.17 ± 2.85	407–413	1.268 ± 0.046	52.80 ± 1.91	1.90
50	394–403	2.517 ± 0.166	52.72 ± 3.47	403–411	1.319 ± 0.164	55.25 ± 6.87	1.91
40	389–400	2.355 ± 0.152	49.63 ± 3.20	400–407	1.524 ± 0.088	64.24 ± 3.70	1.54
30	382–397	2.421 ± 0.099	51.48 ± 1.65	397–405	1.559 ± 0.076	66.33 ± 3.23	1.56
20	377–387	2.357 ± 0.077	50.58 ± 1.65	387–401	1.653 ± 0.079	70.94 ± 3.39	1.41
10	372–281	2.394 ± 0.068	51.83 ± 1.47	381–396	1.777 ± 0.037	76.95 ± 1.60	1.32

high T_c regions of *Figure 1b* are in regime II instead of regime I, Lauritzen's Z test was conducted[3]. While this test is not able to identify the exact growth regime, it is able to indicate whether the regime proposed is reasonable or not. The Z test equation is:

$$Z = z(L/2a)^2 \exp(-4b\sigma\sigma_e T_m^\circ / k\Delta H T_c \Delta T) \exp(2ab\sigma_e / kT_c) \quad (7)$$

where L is the substrate length, z is the ratio of lamellar thickness to length of a monomer unit, and all other symbols have the meanings previously defined. $Z \leqslant 0.01$ corresponds to regime I; $Z \geqslant 1$ indicates growth is in regime II. The 100 wt% iPP crystallized at 493 K has lamellar thickness determined by transmission electron microscopy measurement to be 0.02 μm. For the calculated Z of the 10 wt% iPP crystallized at 493 K, which represents the extreme of the conditions used in this study, to be <0.01, $L/2a$ must be <0.44; this is impossible. If $Z \geqslant 1$, then $L \geqslant a$, which is reasonable. It is concluded that none of the growth rate curves are in regime I.

The absence of a break in the 40 wt% iPP sample and the fact that the regime III slope is smaller than the regime II slope for samples of <40 wt% iPP cannot be explained by the LH theory and are discussed below.

Analysis of kinetic data by the Lauritzen–Hoffman theory: pure iPP samples

The crystal growth rate data in *Figure 1* were analysed using equation (4) with ΔT calculated using the equilibrium melting temperature ($T_m^\circ = 459.5$ K) obtained by the Hoffman–Weeks method[44]. The results are plotted in *Figure 2*. The regime II to III transition occurred at $T_m^\circ / T_c \Delta T f = 2.39 \times 10^{-2}\ K^{-1}$ ($T_c = 413$ K) in *Figure 2* for pure iPP. Clark and Hoffman[22] have prepared the same kinetic plot using data collected from the literature and found the transition occurs within a range of temperatures near 410 K. Monasse and Haudin[26] indicated in their literature survey that the transition point was in the range 406–416 K.

The data in the $T_m^\circ / T_c \Delta T f$ range 2.16–$2.53 \times 10^{-2}\ K^{-1}$ ($T_c = 413$–410 K) represents regime III, while the data in the range 2.53–3.19×10^{-2} ($T_c = 413$–424 K) represent regime II. The slope in regime III is greater than the slope in regime II, which is to be expected based on equations (1) and (2). In the $T_m^\circ / T_c \Delta T f$ range 2.03–$2.16 \times 10^{-2}\ K^{-1}$ ($T_c = 398$–403 K) the growth rate appears to be greater than the regime III straight line predicted by the LH theory. Likewise, in the $T_m^\circ / T_c \Delta T f$ range 3.27–$3.65 \times 10^{-2}\ K^{-1}$ ($T_c = 425$–429 K) the growth rate is greater than the predicted regime II straight line[45,46].

The sensitivity of the kinetic plots to the estimated parameters T_m° and U^* was evaluated to see if appropriate values of these parameters could be found to linearize the data. The T_m° value of 459.5 K obtained[43] and used throughout the data analysis is in good agreement with the accepted literature value of 460.6 K[47]. Although the activation energy has been known to affect the linearity of kinetic plots when T_c is close to T_g[25,43], such an effect was not observed for pure iPP for activation energies ranging from 300 to 2700 cal mol^{-1}. The fact that the change in activation energy has little effect on the linearity of the kinetic plot for the iPP is understandable since in the temperature range of interest in this work, iPP molecules are well above its glass transition temperature (253–263 K). Thus, the migration of iPP molecules is not controlled by the free volume available for the jump but rather the nucleation process.

Sadler proposed the following explanation for the deviations from linearity at extremely large ΔT. Sadler and Gilmer[40,41] criticized some points of the LH theory and proposed a two-dimensional model based on the kinetic roughening surface growth (KRSG) mechanism. Sadler pointed out[36,41] that the one-dimensional model developed by LH for regime III is not based on a nucleation phenomenon, but instead is based on an aggregation phenomenon. The LH theory suggests that, since the supercooling is large in regime III, detachment of polymer molecules from the growth site is not possible once the polymer is deposited on the substrate. However, the driving force for crystallization is still finite in regime III. As pointed out by Sadler[36,39], this constraint against detachment is in violation of microscopic reversibility. Sadler also pointed out that the current regime III theory neglects cavity creation. Thus, the LH regime III theory probably has to be modified according to the two-dimensional growth model with a kinetic roughening step at large supercoolings.

The data at small supercoolings in *Figure 2* represent a deviation from straight-line regime II growth and not a transition to regime I, although Cheng[48] has recently demonstrated that regime II to I transition occurs only for low-molecular-weight iPP. The increase

in growth rate relative to the extrapolated regime II values at small supercoolings may be the result of fractionation of the iPP as explained in another paper in this series[43]. Thus, high temperature crystallization causes fractionation of the polymer and a preferential crystallization of high-molecular-weight chains[49], which grow at a faster rate[45]. Scanning electron microscopy analysis of these samples has provided evidence of this fractionation[50]. Until a sharp fraction of iPP is used in the crystallization study, an exact reason for this increase in growth rate cannot be resolved.

Analysis of kinetic data by the Lauritzen–Hoffman theory: iPP–$C_{32}H_{66}$ samples

The results for iPP–$C_{32}H_{66}$ are presented in *Figures 1* and *2*. Regime II and III growth behaviour are observed for each sample. The transition temperatures established are indicated in *Table 1*. K_g was obtained from the slope of a regression analysis of equation (6) using the data in *Figure 1*; the results are listed in *Table 1*.

$K_{g,III}$ appears to decrease slightly as the polymer concentration decreases from 100 wt%, eventually reaching a constant value at the lower polymer concentrations. $K_{g,II}$ appears to have an even slighter decrease as the polymer concentration is decreased from 100 wt%; however, instead of reaching a plateau at lower concentrations, $K_{g,II}$ appears to increase with further dilution. This increase in $K_{g,II}$ upon dilution is discussed below. The ratio of $K_{g,III}/K_{g,II}$ is approximately 2 (as expected by equation (5)), indicating a regime III to II transition for the high polymer concentration samples. However, the lower polymer concentration samples indicate otherwise. The trend in $K_{g,II}$ indicates the LH regime II mechanism must be modified for dilute iPP–$C_{32}H_{66}$ samples.

The analysis in *Table 1* shows that the Hoffman regime II theory may need modification when the polymer concentration is low. The increase of $K_{g,II}$ with decreasing polymer concentration at low polymer concentrations has been observed in polyethylene single crystals (PESC) crystallized from dilute solutions of paraffin, *p*-xylene, *n*-octane and decaline[33–35,51]. The growth rates at small ΔT in regime II are lower than those extrapolated from larger ΔT in regime II. Toda explains the kinetic curve break and the resulting morphology using an 'impurity' theory, which is a modified form of Frank's model[52].

In correlating the kinetic data with ΔT and concentration in dilute solutions, there are several important factors to be considered[42].

1. Once the initial segment of the polymer chain is attached to the substrate the remaining segments are deposited on the substrate and the patch grows along the substrate surface at a lateral velocity g. However, a growing patch will stop growing when there are no more segments (that is, because the polymer chain has a finite length) or when the growth front encounters an immobile step. The probability of patch growth termination is $1/h^\circ$. The rate of new attachment is i°. The probability $1/h^\circ$ is a function of the nature of the impurity and i° is determined by the faster of two processes: either detachment of impurity from substrate or burying of a defect by initiation of a new stem.

   In the system being studied, this effect can become important when the diluent concentration is increased. $C_{32}H_{66}$, which is rejected from the growth front, is larger than the solvents used in the PESC growth studies of Toda and is more likely to be trapped at the growth surface of the substrate. The trapped diluent will cause the termination described above. Some of the $C_{32}H_{66}$ is inevitably trapped inside the lamellae, a condition that is expected to be more pronounced at high diluent concentrations.
2. Sanchez and DiMarzio[21] developed a dilution-solution theory of polymer crystal growth by introducing cilia nucleation as a crystal growth mechanism. The cilia have been categorized as primary cilia and secondary cilia. Primary cilia are the result of short chain ends that do not participate in crystallization and extend into the solution. Secondary cilia are the result of annihilation of growth steps. Both types of cilia can participate in future crystallization. Toda included cilia nucleation in his model. Cilia nucleation may occur in the current system at high diluent concentrations. The effect of cilia can be lumped into i° because of the similarity in its results. Considering the above factors, the growth rate can be expressed by[42]:

$$G \propto \exp(-K_g/2T_c\Delta T)/(1+b_1/\{1-b_2\exp(-A\Delta T)\})^{1/2} \quad (8)$$

   where A is a parameter proportional to the height and thickness of a monolayer on the growth substrate as defined in ref. 49 and b_1 and b_2 are the fitting parameters for a particular system. The denominator in equation (8) accounts for defects and impurities on the substrate growth surface.

The apparent increase of slope in regime II at high diluent concentration can be explained by equation (8). Since the denominator is greater than one, G is reduced in magnitude when compared with the case of having no defects or impurity. The reduction of growth rate introduced by the denominator increases as supercooling increases. The slope increases at a small ΔT. The model suggests the effect of diluent inclusion on the substrate is most evident as the diluent concentration increases. The crystallinity determined using wide-angle X-ray diffraction[53] for slowly cooled samples showed a decrease as the diluent concentration increased to 50 wt%. This explains why K_g in regime II has the same trend as regime III at high iPP concentrations. The decrease in crystallinity at a higher diluent concentration implies that more diluent was included in the spherulite. The inclusion of diluent coincides with the role of impurity in Toda's model.

The fold surface energy can be calculated from equation (5). The results are listed in *Table 1*. The estimated value of the fold surface energy from both regimes follows the same trends as K_g discussed above.

CONCLUSIONS

The crystallization kinetics of the system iPP–$C_{32}H_{66}$ has been analysed using LH theories. Modification to LH theories was necessary in the regime at low iPP concentrations. Toda's theory[51] was used successfully to explain the kinetic behaviour in regime II. Results indicate that the diluent has an active role in reducing the crystallization rate by inclusion into the polymer crystal.

REFERENCES

1 Hoffman, J. D. and Lauritzen, J. I. *J. Res. Natl Bur. Std.* 1961, **65A**, 297
2 Hoffman, J. D. *SPE Trans.* 1964, **4**, 315
3 Hoffman, J. D., Davis, G. T. and Lauritzen, J. I. in: 'Treatise on Solid State Chemistry' (Ed. N. B. Hannay), Plenum Press, New York, 1976, Chapter 7
4 Lauritzen, J. I. and Hoffman, J. D. *J. Appl. Phys.* 1973, **44**, 4340
5 Guttman, C. M., DiMarzio, E. A. and Hoffman, J. D. *Polymer* 1981, **22**, 1466
6 Hoffman, J. D. *Polymer* 1982, **23**, 656
7 Hoffman, J. D. *Polymer* 1983, **24**, 3
8 Hoffman, J. D. *Polymer* 1985, **26**, 803
9 Hoffman, J. D. and Miller, R. L. *Macromolecules* 1988, **21**, 3038
10 Sanchez, I. C. *J. Macromol. Sci.-Rev. Macromol. Chem.* 1974, **C10**, 113
11 Nedkov, E. and Mihajlov, M. *J. Polym. Sci. C* 1972, **38**, 33
12 Ong, C. J. and Price, F. P. *J. Polym. Sci., Polym. Symp. Edn* 1978, **63**, 45, 59
13 Galeski, A., Barrczak, Z. and Pracella, M. *Polymer* 1986, **27**, 537
14 Yeh, G. S. Y. and Lambert, S. L. *J. Polym. Sci., A-2* 1972, **10**, 1183
15 Martuscelli, E., Riva, F., Sellitti, C. and Silvestre, C. *Polymer* 1985, **26**, 270
16 Lauritzen, J. I. and Hoffman, J. D. *J. Res. Natl Bur. Std.* 1960, **64A**, 73
17 Lauritzen, J. I. and Passaglia, E. *J. Res. Natl Bur. Std.* 1967, **71A**, 261
18 Frank, F. C. and Tosi, M. *Proc. R. Soc.* 1961, **A263**, 323
19 Price, F. P. *J. Polym. Sci.* 1960, **42**, 49
20 Sanchez, I. C. and DiMarzio, E. A. *J. Res. Natl Bur. Std.* 1972, **76A**, 213
21 Sanchez, I. C. and DiMarzio, E. A. *Macromolecules* 1971, **4**, 677
22 Clark, E. J. and Hoffman, J. D. *Macromolecules* 1984, **17**, 76
23 Allen, R. C. and Mandelkern, L. *Polym. Bull.* 1987, **17**, 473
24 Rensch, G. J., Phillips, P. J., Vantansever, N. and Gonzalez, V. A. *J. Polym. Sci., Polym. Phys. Edn* 1986, **24**, 1943
25 Lovinger, A. L., Davis, D. D. and Padden, F. J. *Polymer* 1985, **26**, 1595
26 Monasse, B. and Haudin, J. M. *Colloid Polym. Sci.* 1985, **263**, 822
27 Mandelkern, L. *J. Appl. Phys.* 1955, **26**, 443
28 Boon, J. and Azcue, J. M. *J. Polym. Sci.* 1968, **6**, 885
29 Chaturvedi, P. N. *Makromol. Chem.* 1987, **188**, 433
30 Keith, H. D. and Padden, F. J. *J. Appl. Phys.* 1964, **35**, 1270, 1286
31 Keith, H. D., Padden, F. J. and Russell, T. P. *Macromolecules* 1989, **22**, 666
32 Toda, A., Miyaji, H. and Kiho, H. *Polymer* 1986, **27**, 1505
33 Organ, S. J. and Keller, A. *J. Polym. Sci., Polym. Phys. Edn* 1986, **24**, 2319
34 Cooper, M. and Manley-St. John, R. *Macromolecules* 1975, **8**, 219
35 Leung, W. M., Manley-St. John, R. and Panaras, A. R. *Macromolecules* 1985, **18**, 760
36 Sadler, D. M. *Polymer* 1983, **24**, 1401
37 Sadler, D. M. *Polym. Commun.* 1986, **27**, 140
38 Sadler, D. M. *J. Chem. Phys.* 1987, **87**, 1771
39 Sadler, D. M. *Polymer* 1987, **28**, 1440
40 Sadler, D. M. and Gilmer, G. H. *Polymer* 1984, **25**, 1446
41 Sadler, D. M. and Gilmer, G. H. *Phys. Rev. Lett.* 1986, **56**, 2708
42 Toda, A., Kiho, H., Miyaji, H. and Asai, K. *J. Phys. Soc. Jpn* 1985, **54**, 1411
43 Wang, Y. F. and Lloyd, D. R. *Polymer* in press
44 Hoffman, J. D. and Weeks, J. J. *J. Res. Natl Bur. Stds* 1962, **66A**, 13
45 Philips, P. J. and Vatansever, N. *Macromolecules* 1987, **20**, 2138
46 Cheng, S. Personal communication
47 Wunderlich, B. 'Macromolecular Physics', Vol. 3, Academic Press, New York, 1980
48 Cheng, S. Personal communication
49 Wunderlich, B. *Faraday Disc. R. Soc. Chem.* 1979, **68**, 239
50 Wang, Y. F. and Lloyd, D. R. unpublished results
51 Toda, A. *Polymer* 1987, **28**, 1645
52 Frank, F. C. *J. Cryst. Growth* 1974, **22**, 233
53 Ye, Q. H. *Master's Thesis* University of Texas at Austin, TX, 1990